Observation of the $\phi \to \eta'\gamma$ decay with four charged particles and photons in the final state

R.R. Akhmetshin[*], E.V.Anashkin[*], M.Arpagaus[*], V.M.Aulchenko[*†], V.Sh.Banzarov[*], L.M.Barkov[*†], N.S.Bashtovoy[*], A.E.Bondar[*†], D.V.Bondarev[*], A.V.Bragin[*], D.V.Chernyak[*], S.I.Eidelman[*†], G.V.Fedotovitch[*†], N.I.Gabyshev[*], A.A.Grebeniuk[*], D.N.Grigoriev[*], V.W.Hughes[‡], F.V.Ignatov[*†], P.M.Ivanov[*], S.V.Karpov[*], V.F.Kazanin[*†], B.I.Khazin[*†], I.A.Koop[*], M.S.Korostelev[*], P.P.Krokovny[*†], L.M.Kurdadze[*†], A.S.Kuzmin[*†], I.B.Logashenko[*], P.A.Lukin[*], K.Yu.Mikhailov[*†], I.N.Nesterenko[*], V.S.Okhapkin[*], A.V.Otboev[*], E.A.Perevedentsev[*†], A.S.Popov[*†], T.A.Purlatz[*†], S.I.Redin[*], N.I.Root[*†], A.A.Ruban[*], N.M.Ryskulov[*], A.G.Shamov[*], Yu.M.Shatunov[*], B.A.Shwartz[*†], A.L.Sibidanov[*†], V.A.Sidorov[*], A.N.Skrinsky[*], V.P.Smakhtin[*], I.G.Snopkov[*], E.P.Solodov[*†], P.Yu.Stepanov[*], A.I.Sukhanov[*], J.A.Thompson[§], V.M.Titov[*], A.A.Valishev[*], Yu.V.Yudin[*], S.G.Zverev[*]

February 7, 2008

[*]Budker Institute of Nuclear Physics, Novosibirsk, 630090, Russia
[†]Novosibirsk State University, Novosibirsk, 630090, Russia
[‡]Yale University, New Haven, CT 06511, USA
[§]University of Pittsburgh, Pittsburgh, PA 15260, USA

Abstract

Using 11.6 pb^{-1} of data collected in the energy range 0.864-1.06 GeV by CMD-2 at VEPP-2M, the rare decay mode $\phi \to \eta'\gamma$ was observed via the decay chain $\eta' \to \pi^+\pi^-\eta$, $\eta \to \pi^+\pi^-\pi^0$ or $\eta \to \pi^+\pi^-\gamma$. The following branching ratio was obtained:

$$Br(\phi \to \eta'\gamma) = (4.9^{+2.2}_{-1.8} \pm 0.6) \cdot 10^{-5}\,.$$

1 Introduction

Measurements of radiative decays of light vector mesons provide good tests of the quark model and extend our understanding of SU(3) symmetry breaking [1, 2]. The discovery of the rare decay $\phi \to \eta'\gamma$ by CMD-2 [3] has brought the last piece into the otherwise complete mosaic of radiative dipole magnetic transitions between light vector and pseudoscalar mesons. This observation was later confirmed by the SND group [4]. Recently CMD-2 presented an improved measurement of the rate of the $\phi \to \eta'\gamma$ decay [5] based on the total data sample accumulated in the ϕ-meson energy range. The first preliminary results by the KLOE collaboration on the $Br(\phi \to \eta'\gamma)$ value reported recently [6] are consistent with those from CMD-2 and SND within the experimental uncertainties.

Because of the rather low probability of the studied decay as well as serious background problems resulting in strict selection criteria, none of the above measurements have good statistical precision. One way to increase a sample of $\eta'\gamma$ events is to use other decay modes of the η' and η mesons. In most of the previous papers [3, 4, 5, 6] events of the decay $\phi \to \eta'\gamma$ were selected in the mode $\eta' \to \pi^+\pi^-\eta$, $\eta \to \gamma\gamma$. The pure neutral decay chain $\eta' \to \pi^0\pi^0\eta$, $\eta \to \gamma\gamma$ has been also used by the KLOE group [6]. In this paper we study the decay $\phi \to \eta'\gamma$ with the CMD-2 detector at VEPP-2M in the channels:

$$\phi \to \eta'\gamma\,, \quad \eta' \to \eta\pi^+\pi^-\,, \qquad \eta \to \pi^+\pi^-\pi^0 \quad \text{or} \tag{1}$$

$$\phi \to \eta'\gamma\,, \quad \eta' \to \eta\pi^+\pi^-\,, \qquad \eta \to \pi^+\pi^-\gamma. \tag{2}$$

The analysis is based on the data sample collected in three scans of the c.m.energy range from 0.984 to 1.060 GeV performed in winter 1997–1998. The total integrated luminosity of about 11.6 pb^{-1} corresponds to approximately 16 million ϕ meson decays.

The general purpose detector CMD-2 has been described in detail elsewhere [7]. It consists of a drift chamber (DC) [8] and a proportional

Z-chamber [9], both used for the trigger, and both inside a thin (0.4 X_0) superconducting solenoid with a field of 1 T.

The barrel calorimeter [10] which is placed outside the solenoid, consists of 892 CsI crystals of $6 \times 6 \times 15$ cm^3 size and covers polar angles from 46° to 134°. The energy resolution for photons is about 9% in the energy range from 50 to 600 MeV. The angular resolution is about 0.02 radians.

The end-cap calorimeter [11] which is placed inside the solenoid, consists of 680 BGO crystals of $2.5 \times 2.5 \times 15$ cm^3 size and covers forward-backward polar angles from 16° to 49° and from 131° to 164°. The energy and angular resolution varies from 8% to 4% and from 0.03 to 0.02 radians respectively for the photons in the energy range from 100 to 700 MeV.

The luminosity was determined from Bhabha scattering events at large angles [12].

2 Data analysis

The specific signature of the processes (1) and (2) is the final state with four charged pions coming from the interaction region and two or more photons. It is well known that the ϕ meson decays do not provide such a signature with the exception of the following decays into kaons:

$$\phi \rightarrow K^0_S K^0_L,\ K^0_S \rightarrow \pi^+\pi^-,\ K^0_L \rightarrow \pi^+\pi^-\pi^0 \quad \text{and} \tag{3}$$

$$\phi \rightarrow K^+K^-,\ K^\pm \rightarrow \pi^\pm\pi^+\pi^-,\ K^\mp \rightarrow \pi^\mp\pi^0. \tag{4}$$

However, because of the large lifetime of kaons charged particles originating from the kaon decays have a broad distribution of the impact parameter with respect to the interaction point. It is this feature which will be used to suppress this background and control the contamination of the final event sample.

Another background reaction is $e^+e^- \rightarrow \omega\pi^0$, $\omega \rightarrow \pi^+\pi^-\pi^0$ followed by the Dalitz decay of one of the pions: $\pi^0 \rightarrow e^+e^-\gamma$. In this case the distribution of the minimum space angle between the charged tracks has a characteristic peak at small angles.

We selected events with four charged tracks coming from the interaction region: the maximum impact parameter of the tracks $d = \max_{i=1}^{4}(r_{min_i})$ is less than 1 cm and the vertex coordinate along the beam axis z_{vert} is within ±10 cm. For better reconstruction efficiency, tracks were also required to cross at least two superlayers of the drift chamber: $|\cos\theta| < 0.8$. Two or more photons have to be detected in the calorimeter. For the selected events the kinematic fit was performed taking into account energy — momentum conservation and assuming all charged particles to be pions.

One of the main problems in the analysis is additional ("fake") photons induced by the products of nuclear interactions of charged pions in the detector material. The following method was used to suppress such fake photons. In the kinematic fit the energy resolution of photons was loosened to the value $\sigma_{E_\gamma} = E_\gamma + 20$ MeV. Thus, the photon energy was allowed to vary in a wide range during the fit. As the first step, the fit was performed in the hypothesis of the $\pi^+\pi^-\pi^+\pi^-\gamma\gamma$ final state. For events with more than two detected photons ($N_\gamma^{det} > 2$) the fit was repeated for all possible pairs of photons and the pair with the smallest $\chi^2_{4\pi2\gamma}$ characterizing the fit quality was selected. Then, for these events, the assumption of the $\pi^+\pi^-\pi^+\pi^-\gamma\gamma\gamma$ state was tested. For events with $N_\gamma^{det} > 3$, the combination of three photons with the smallest $\chi^2_{4\pi3\gamma}$ was selected. Finally, the signature $\pi^+\pi^-\pi^+\pi^-\gamma\gamma$ or $\pi^+\pi^-\pi^+\pi^-\gamma\gamma\gamma$ was assigned to the event depending on whether the magnitude of $\chi^2_{4\pi2\gamma}$ or $\chi^2_{4\pi3\gamma}$ was smaller. Then the requirement on the fit quality $\chi^2 = \min(\chi^2_{4\pi2\gamma}, \chi^2_{4\pi3\gamma})$ was applied: $\chi^2/\text{n.d.f} < 10/4$. Events with the reconstructed photon energy below 30 MeV were rejected from the subsequent analysis.

The background coming from the decay $\phi \to K^+K^-$, in which products of kaon nuclear interaction scatter back to the drift chamber and induce two extra tracks or one of the kaon decays via the $K^\pm \to \pi^\pm\pi^+\pi^-$ channel, accompanied by fake photons, was suppressed using ionization losses of the tracks (see [8, 13] for more detail). Requiring $E_{4\pi}/2E_{beam} > 0.7$, where $E_{4\pi} = \sum_{i=1}^{4}\sqrt{\vec{p}_i^{\,2} + m_\pi^2}$ is the total energy of the tracks, additional suppression of this type of the background was achieved.

To suppress the background reaction $e^+e^- \to \omega\pi^0$, where $\omega \to \pi^+\pi^-\pi^0$ and one of the neutral pions decays to $e^+e^-\gamma$, a previously tested procedure for e/π-separation (see [14, 15] for details) was employed. In this procedure, using the data samples of $e^+e^- \to \pi^+\pi^-\pi^0$ and $e^+e^- \to e^+e^-\gamma$ events, the probability density functions for the parameter $E_{CsI}/|\vec{p}|$ were obtained for both particle types (e/π) and signs ($+/-$): f_{π^+}, f_{π^-}, f_{e^+} and f_{e^-}. Here E_{CsI} is the energy deposition in the CsI calorimeter and $\vec{p}$ is the momentum of the particle with a track matching the cluster in CsI. Then the probability for the pair of tracks to be pions was defined: $W_{\pi^+\pi^-} = f_{\pi^+}f_{\pi^-}/(f_{\pi^+}f_{\pi^-} + f_{e^+}f_{e^-})$. Figure 1 shows the distribution of $W_{\pi^+\pi^-}$ for the events of the processes $e^+e^- \to e^+e^-\gamma$ and $e^+e^- \to \pi^+\pi^-\pi^0$ demonstrating clear separation of the two types of the processes. Since the decay $\pi^0 \to e^+e^-\gamma$ features a small space angle between e^+e^-, we searched for a pair of oppositely charged particles with a minimum space angle ψ_{min}. The probability $W_{\pi^+\pi^-}$ was calculated for this pair. After that, the condition $W_{\pi^+\pi^-} > 0.5$ suppressed about 70% of the $\omega\pi^0$ events. In addition, ionization losses dE/dx were used to reject $\omega\pi^0$ events with a low momentum of e^+e^- [13].

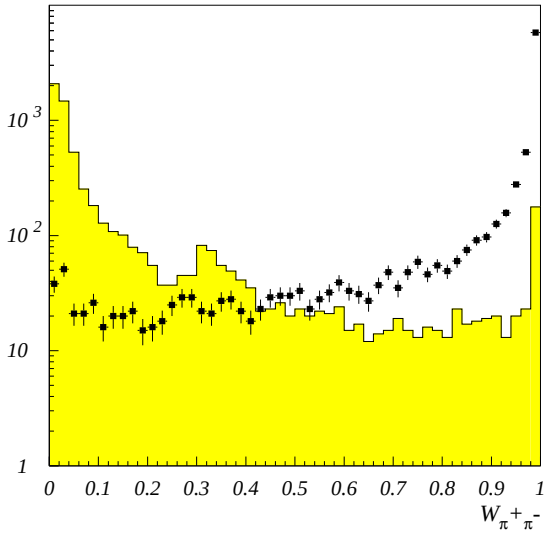

Figure 1: e/π separation probability. Distribution of $W_{\pi^+\pi^-}$ for the events of the processes $e^+e^- \to e^+e^-\gamma$ (histogram) and $e^+e^- \to \pi^+\pi^-\pi^0$ (points with errors)

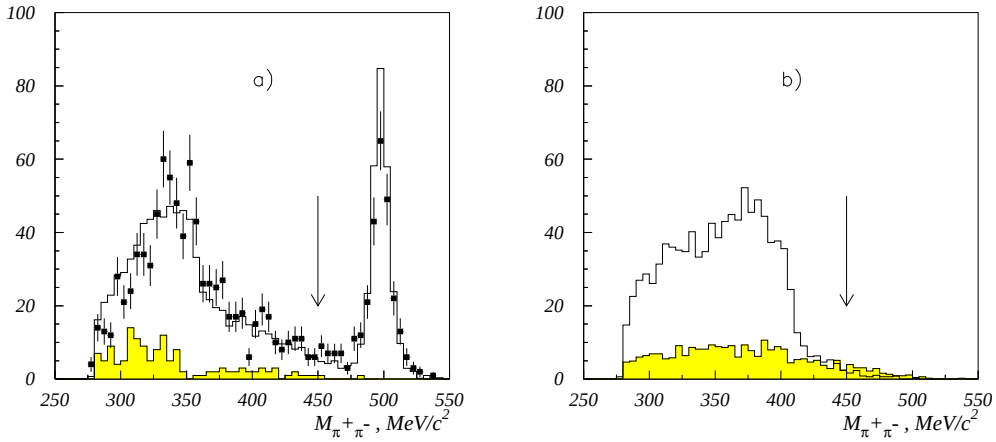

Figure 2: The invariant mass $M_{\pi^+\pi^-}$. a) Points with error bars — data; transparent histogram — MC of the process (3); hatched histogram — MC of the reaction (4); b) Simulation of the $\phi \to \eta'\gamma$ decay; transparent histogram — decay $\eta \to \pi^+\pi^-\pi^0$; hatched histogram — decay $\eta \to \pi^+\pi^-\gamma$

About 250 events were selected after application of the criteria described above. For these events the distribution of the invariant mass of the pairs of charged pions $M_{\pi^+\pi^-}$ is shown in Fig.2a) by the black squares with error bars (four entries from one event). The transparent histogram in this Figure presents the distribution obtained by the complete Monte Carlo simulation (MC) of the CMD-2 detector [16] for the process (3), while the hatched histogram is the MC of the reaction (4). The number of events in $K_S^0K_L^0$ MC samples corresponds to approximately the same integrated luminosity as in our data. For comparison, in Fig.2b) the same distributions of $M_{\pi^+\pi^-}$ are shown for the simulation of the decays (1) and (2).

As one can see from Fig. 2a), the main contribution to the selected events comes from the process $\phi \to K_S^0K_L^0$ followed by the decays $K_S^0 \to \pi^+\pi^-$ and $K_L^0 \to \pi^+\pi^-\pi^0$. The requirement that $M_{\pi^+\pi^-} < 450\,\mathrm{MeV}/c^2$ for each of the four possible $\pi^+\pi^-$ pairs efficiently rejects the $K_S^0K_L^0$ events and does not influence the events of the decay under study (see Fig. 2b)). After that only 23 events survive.

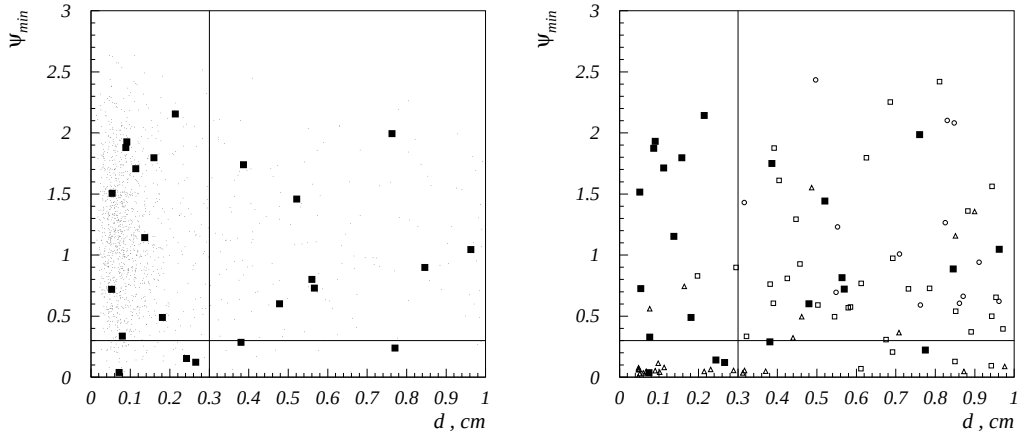

Figure 3: The minimum space angle between the tracks versus the maximum impact parameter of the tracks. Black squares in both Figures present the experimental data; a) points are the MC of the decays (1) and (2); b) $\circ$ is the MC of $K_S^0K_L^0$ events; $\square$ is the MC of K^+K^- events; $\triangle$ is the MC of $\omega\pi^0$ events. The number of events in the MC samples of charged and neutral kaons and the number of simulated $\omega\pi^0$ events exceed the number of events of these reactions expected at our integrated luminosity by a factor of 10 and 4 respectively

To complete separation of the $\eta'\gamma$ events and estimate the remaining background from the $\omega\pi^0$, $K_S^0K_L^0$ and K^+K^- events, the distributions of the minimum space angle between the tracks and the maximum impact parameter of the tracks were analyzed for 23 selected events. In Fig.3a) the scatter plot of ψ_{min} versus d is shown for the experimental data in comparison to the simulation of the decays (1) and (2). In Fig.3b) the same experimental data are compared to the MC of the background events $K_S^0K_L^0$, K^+K^- and $\omega\pi^0$.

It is obvious from these Figures, that events of the decay under study contribute to the region of small impact parameters and feature a broad distribution of ψ_{min}. The background events $\omega\pi^0$ fall mainly in the region of small angles: $\psi_{min} \lesssim 0.2$, while the events with neutral and charged kaons have approximately flat distribution of the maximum impact parameters of tracks with $d \gtrsim 0.3$ cm. Correspondingly, the plane of the parameters ψ_{min} and d was subdivided into three following regions:

1. the $\eta'\gamma$ region: $\psi_{min} > 0.3$ and $d < 0.3$ cm;
2. the $\omega\pi^0$ region: $\psi_{min} < 0.3$ and $d < 0.3$ cm;
3. the $K\bar{K}$ region: $\psi_{min} > 0.3$ and $d > 0.3$ cm.

The fourth region ($\psi_{min} > 0.3$ and $d > 0.3$ cm) contains a small contribution from all three background reactions.

Ten candidate events of the $\phi \to \eta'$ decay were selected in the $\eta'\gamma$ region: $\tilde{N}_{\eta'\gamma} = 10$. For these events the distribution of the missing mass for the pair of charged pions and the photon with the energy closest to that of the monochromatic photon from the decay $\phi \to \eta'\gamma$ is shown in Fig. 4. The MC spectrum in this Figure was obtained as a sum of the contributions of the processes (1) and (2) with the numbers of events proportional to the corresponding decay probabilities. One can see that the experimental data agree well with the simulation.

The number of background events was found to be: $\tilde{N}_{\omega\pi^0} = 3$ and $\tilde{N}_{K\bar{K}} = 8$ in the regions $\omega\pi^0$ and $K\bar{K}$ respectively.

Figure 5a) shows the distribution of the missing mass of all four charged pions versus the maximum impact parameter of the tracks for the events, which were selected under the condition $\psi_{min} > 0.3$. Good agreement is observed between the Monte Carlo simulation of the signal and the experimental data for $d < 0.3$ cm. In Fig. 5b the same distribution of the experimental data is shown in comparison to the simulation of the background processes (3) and (4). These Figures provide one more verification of our assumption that the $\eta'\gamma$ events contribute to the region of small impact parameters,

while events with the decays of neutral and charged kaons have tracks which originate at rather large distances from the interaction point.

The following probabilities to observe the background events $\omega\pi^0$, $K^0_S K^0_L$ and K^+K^- in the $\eta'\gamma$ region, were obtained from the MC:

$$W_{\omega\pi^0} = \frac{N_{\omega\pi^0}(\psi_{min} > 0.3\,, d < 0.3\,\mathrm{cm})}{N_{\omega\pi^0}(\psi_{min} < 0.3\,, d < 0.3\,\mathrm{cm})} = 0.14 \pm 0.10\,,$$

$$W_{K\bar{K}} = \frac{N_{K\bar{K}}(\psi_{min} > 0.3\,, d < 0.3\,\mathrm{cm})}{N_{K\bar{K}}(\psi_{min} > 0.3\,, d > 0.3\,\mathrm{cm})} = 0.10 \pm 0.05\,.$$

Using these probabilities and the numbers of events $\tilde{N}_{\omega\pi^0}$ and $\tilde{N}_{K\bar{K}}$, the background contribution into ten candidate events $\tilde{N}_{\eta'\gamma}$ was estimated. Finally, the number of the $\eta'\gamma$ events was calculated from the formula:

$$N_{\eta'\gamma} = \tilde{N}_{\eta'\gamma} - \tilde{N}_{K\bar{K}} W_{K\bar{K}} - \tilde{N}_{\omega\pi^0} W_{\omega\pi^0} = 8.8^{+3.8}_{-3.2}\,.$$

The error is determined by the statistics of selected events only, as well as the background contribution whereas the errors of the probabilities $\mathrm{W}_{\omega\pi^0}$ and $\mathrm{W}_{K\bar{K}}$ will be included in the systematic uncertainty. Here we did not take into account the possibility to observe $\eta'\gamma$ events in the background regions as well as the probabilities to detect the $\omega\pi^0$ events in the region $K\bar{K}$ and vice versa. All these effects contribute less that 3% into $N_{\eta'\gamma}$ and were also included into the systematic uncertainty.

The detection efficiency was obtained using the Monte Carlo simulation of the processes (1) and (2): $\epsilon_{3\pi} = 0.097 \pm 0.003$ and $\epsilon_{\pi\pi\gamma} = 0.091 \pm 0.003$.

The process (3) was also used for the normalization and calculation of the $\phi \to \eta'\gamma$ decay probability. To select $K^0_S K^0_L$ events, conditions similar to those for $\eta'\gamma$ were used with one exception. We required $M_{\pi^+\pi^-} > 450\,\mathrm{MeV}/c^2$ for at least one $\pi^+\pi^-$ pair. Note that this condition effectively suppresses the process (4). The selection efficiency was determined from MC: $\epsilon_{K^0_S K^0_L} = (4.9 \pm 0.3) \cdot 10^{-4}$. The number of detected events is $N_{K^0_S K^0_L} = 216$.

The relative probability of the decay $\phi \to \eta'\gamma$ was calculated using the formula:

$$\begin{aligned} \frac{Br(\phi \to \eta'\gamma)}{Br(\phi \to K^0_S K^0_L)} &= \frac{N_{\eta'\gamma}}{N_{K^0_S K^0_L}} \cdot \frac{Br(K^0_S \to \pi^+\pi^-) Br(K^0_L \to \pi^+\pi^-\pi^0)}{Br(\eta' \to \pi^+\pi^-\eta)} \\ \times \quad & \frac{\epsilon_{K^0_S K^0_L}}{\epsilon_{3\pi} Br(\eta \to \pi^+\pi^-\pi^0) + \epsilon_{\pi\pi\gamma} Br(\eta \to \pi^+\pi^-\gamma)} \\ = \quad & (1.46^{+0.64}_{-0.54} \pm 0.18) \cdot 10^{-4}\,. \end{aligned} \tag{5}$$

The systematic uncertainty arises from the following contributions: 6.7% comes from the uncertainties in determination of the detection efficiencies $\epsilon_{3\pi}$,

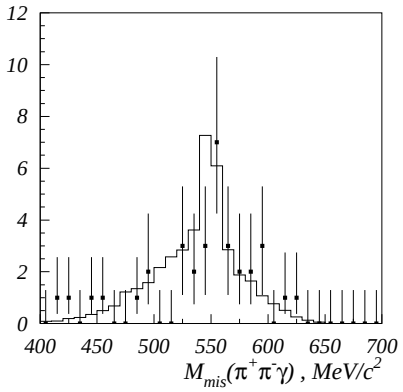

Figure 4: The missing mass for the pair of pions and the photon with the energy closest to that of the monochromatic photon from the decay $\phi \to \eta'\gamma$; histogram — Monte Carlo, black squares with error bars — data

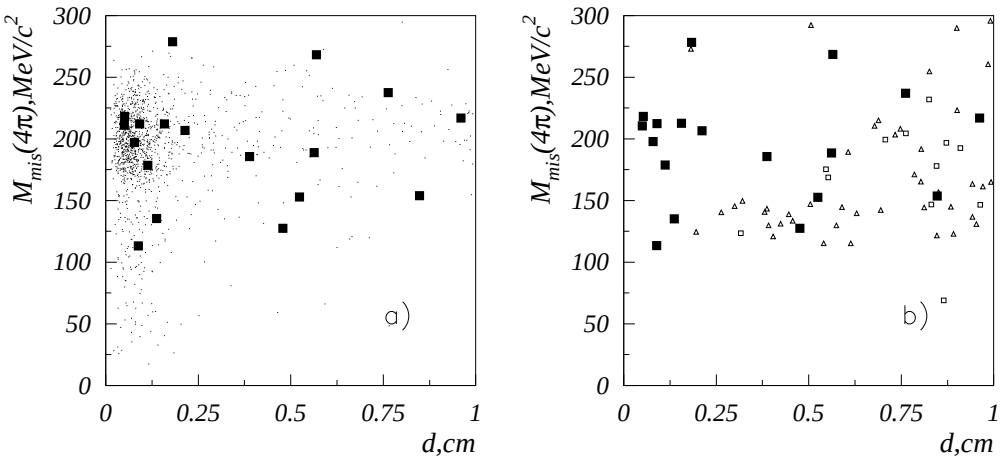

Figure 5: The missing mass of 4π versus the maximum impact parameter of the tracks. The black squares in both pictures – experimental data; (a) dots – sum of Monte Carlo of the processes (1) and (2); (b) light squares – MC of the $\phi \to K^0_S K^0_L$ decay, light triangles – MC of the $\phi \to K^+K^-$ decay

Table 1: Summary of the $\phi \to \eta'\gamma$ decay rate measurements

Experiment	$\eta'\gamma$ decay mode	$\frac{Br(\phi\to\eta'\gamma)}{Br(\phi\to\eta\gamma)}$, 10^{-3}	$\frac{Br(\phi\to\eta'\gamma)}{Br(\phi\to K^0_S K^0_L)}$, 10^{-4}	$Br(\phi \to \eta'\gamma)$, 10^{-5}
CMD-2 [3]	$\eta' \to \pi^+\pi^-\eta$, $\eta \to \gamma\gamma$	$9.5^{+5.2}_{-4.0} \pm 1.4$		$12.0^{+7.0}_{-5.0} \pm 1.8$
SND [4]	$\eta' \to \pi^+\pi^-\eta$, $\eta \to \gamma\gamma$			$6.7^{+3.4}_{-2.9} \pm 1.0$
CMD-2 [5], includes [3]	$\eta' \to \pi^+\pi^-\eta$, $\eta \to \gamma\gamma$	$6.5^{+1.7}_{-1.5} \pm 0.8$		$8.2^{+2.1}_{-1.9} \pm 1.1$
KLOE [6]	$\eta' \to \pi^+\pi^-\eta$, $\eta \to \gamma\gamma$	$7.1 \pm 1.6 \pm 0.3$		$8.9 \pm 2.0 \pm 0.6$
	$\eta' \to \pi^0\pi^0\eta$, $\eta \to \gamma\gamma$	$6.8^{+3.2}_{-2.5} \pm 0.9$		
CMD-2, this work	$\eta' \to \pi^+\pi^-\eta$, $\eta \to \pi^+\pi^-\pi^0$ or $\eta \to \pi^+\pi^-\gamma$		$1.46^{+0.64}_{-0.54} \pm 0.18$	$4.9^{+2.2}_{-1.8} \pm 0.6$

$\epsilon_{\pi\pi\gamma}$ and $\epsilon_{K^0_S K^0_L}$; 7% comes from the stability of the selection criteria, 6.4% is due to the background subtraction and 4.1% comes from the uncertainties in the decay probabilities used in the Eq.(5). All decay probabilities were taken from [17]. The overall systematic uncertainty is 12.3%.

Finally, taking the value of $Br(\phi \to K^0_S K^0_L)$ from [17], the following branching ratio was obtained:

$$Br(\phi \to \eta'\gamma) = (4.9^{+2.2}_{-1.8} \pm 0.6) \cdot 10^{-5} \ .$$

The energy behaviour of the cross section calculated using ten selected events does not contradict the shape expected for the sum of the ϕ meson and non-resonant background.

3 Discussion

The currently available data on the measurements of the $\phi \to \eta'\gamma$ decay probability are shown in Table 1 in comparison to our result. The value of the decay probability $Br(\phi \to \eta'\gamma)$ obtained in our work is lower than that in [4, 5, 6], but is consistent with their results within a statistical uncertainty.

The previous CMD-2 measurement of $Br(\phi \to \eta'\gamma)$ in the decay chain $\phi \to \eta'\gamma$, $\eta' \to \pi^+\pi^-\eta$ and $\eta \to \gamma\gamma$ [5] is based on the data set, which is

statistically independent of our data sample. Analysis of the sources of systematic errors in both measurements also shows that they are uncorrelated. Thus, to improve the accuracy of the branching ratio determination, we can combine both results:

$$Br(\phi \to \eta'\gamma)_{\text{CMD-2}} = (6.4 \pm 1.6) \cdot 10^{-5} \,.$$

The authors are grateful to the staff of VEPP-2M for excellent performance of the collider, to all engineers and technicians who participated in the design, commissioning and operation of CMD-2.

REFERENCES

1. P.J.O'Donnell, Rev. Mod. Phys. **53** (1981) 673.
2. M.Benayoun *et al.,* Phys. Rev. **D59** (1999) 114027.
3. R.R.Akhmetshin *et al.,* Phys. Lett. **B415** (1997) 445.
4. V.M.Aulchenko *et al.,* JETP Lett. **69** (1999) 97.
5. R.R.Akhmetshin *et al.,* Phys. Lett. **B473** (2000) 337.
6. KLOE collaboration, Contributed paper to the XXX International Conference on High Energy Physics, Osaka 27 Jul – 2 Aug 2000; hep-ex/0006036.
7. G.A.Aksenov *et al.*, Preprint Budker INP 85-118, Novosibirsk, 1985. E.V.Anashkin *et al.*, ICFA Instr. Bulletin **5** (1988) 18.
8. F.V.Ignatov *et al.*, Preprint Budker INP 99-64, Novosibirsk, 1999.
9. E.V.Anashkin *et al.*, Preprint Budker INP 99-84, Novosibirsk, 1999.
10. V.M.Aulchenko *et al.*, Nucl. Instr. and Meth. **A366** (1993) 53.
11. D.N.Grigoriev *et al.*, IEEE Trans. Nucl. Sci. **42** (1995) 505.
12. R.R.Akhmetshin *et al.*, Preprint Budker INP 99-11, Novosibirsk, 1999.
13. R.R.Akhmetshin *et al.*, Phys. Lett. **B491** (2000) 81; hep-ex/0008019.
14. R.R.Akhmetshin *et al.*, Phys. Lett. **B475** (2000) 190; hep-ex/9912020.
15. R.R.Akhmetshin *et al.*, Preprint Budker INP 99-97, Novosibirsk, 1999.
16. E.V.Anashkin *et al.*, Preprint Budker INP 99-1, Novosibirsk, 1999.
17. D.E.Groom *et al.,* Eur. Phys. J. **C15** (2000) 1.